Observation of Charge-Density Wave Domains on the Cr(110) Surface by Low-Temperature Scanning Tunneling Microscopy

K.-F. Braun, S. Fölsch,* G. Meyer, and K.-H. Rieder

Institut für Experimentalphysik, Freie Universität Berlin, Arnimallee 14, D-14195 Berlin, Germany

(Received 11 April 2000)

We have studied the Cr(110) surface with low-temperature scanning tunneling microscopy at 6 to 145 K. For tunneling voltages below ± 150 mV we observe a surface charge-density wave (CDW) with a wavelength of 42 Å and wave fronts aligned with the [001] in-plane direction. The observed wave pattern is identified as the surface projection of the bulk CDW's arising from the spin-density wave ground state of Cr with the **Q** vector parallel to [100] and [010], respectively. The bulk CDW with **Q** parallel to the [001] in-plane direction appears, however, to be strongly suppressed at the Cr(110) surface.

PACS numbers: 75.30.Pd, 61.16.Ch, 75.30.Fv

The spin-density wave ground state of the itinerant antiferromagnet chromium [1,2] is the subject of long-standing scientific interest concerning its fundamental nature and, more recently, its technological implications [2]. Below the Néel temperature ($T_N = 311$ K) bulk Cr exhibits static spin-density waves (SDW) due to wave vector nesting of the electron and hole Fermi surfaces [3]. As a result of the nesting condition, the wave vector **Q** is incommensurate with the lattice and may point along any of the three $\langle 100 \rangle$ directions of the bcc Cr lattice. The SDW may be either longitudinal ($\mathbf{S} \parallel \mathbf{Q}$ below T_{SF}) or transversal ($\mathbf{S} \perp \mathbf{Q}$ above T_{SF}) in character, where **S** denotes the spin polarization and $T_{SF} = 123$ K is the spin flip transition temperature. The SDW is accompanied by a strain wave and a charge-density wave (CDW) with half the period of the SDW [4–7]. As an important issue to technological applications, SDW's play a crucial role in the giant magnetoresistance effect [8] in Cr/Fe superlattices which is triggered by oscillatory magnetic coupling across the antiferromagnetic Cr spacer layer [9,10]. Up to now, all experimental information available on the structural features of SDW's and CDW's in bulk Cr or in thin Cr films is based on spatially averaging approaches such as neutron [1] and x-ray diffraction [1,2,5–7] or spectroscopic techniques [11,12]. In this Letter, we present for the first time a local probe study of CDW's at a Cr surface by low-temperature scanning tunneling microscopy (LT-STM). We show that the antiferromagnetic (AFM) surface domain structure of Cr can be imaged indirectly via CDW's accompanying the SDW ground state. Besides the recently published work of Scholl *et al.* [13], this is—to our knowledge—the only experimental study to date that gives access to the microscopic domain structure of an AFM surface on the nanometer scale. The present observations are also remarkable in the sense that they arise from the surface projection of a 3D bulk CDW. In contrast, only surface charge-density modulations associated with surface-localized states [14,15] or with CDW's in quasi-1D [16] or 2D layered materials [17] have been observed by STM so far.

The experiments were carried out with a homebuilt ultrahigh vacuum (UHV) LT-STM which operated at temperatures between 6 and 300 K. The Cr(110) surface was cleaned by extensive Ne^+ sputtering and simultaneous annealing cycles up to 970 K (1 keV, ~ 4 μA). It is known from literature that UHV cleaning of Cr surfaces is a tedious task owing to persistent segregation of bulk contaminants [18]. In the present case, the applied treatment finally yielded a well-ordered surface with terraces typically 600 Å in size and segregated contaminants (predominantly nitrogen [18]) reduced to an estimated surface concentration below $\sim 8\%$. The exemplary STM image in Fig. 1(a) was taken in constant current mode at 6 K (750 Å $\times$ 560 Å, 1000 MΩ tunneling resistance, $U_t = -1$ V referring to the sample with respect to the tip) and shows seven terraces which are separated by monatomic steps preferentially aligned with the [001] direction and the close-packed $[\bar{1}11]$ direction. The crystallographic orientation and the centered rectangular unit cell is inferred from the inset in Fig. 1(a) (20 Å $\times$ 18 Å, 0.1 MΩ, $U_t = 10$ mV) demonstrating atomic resolution of the Cr(110) surface. Residual surface contaminants are imaged as depletions on top of the flat terraces. It is noted that these contaminants tend to form elongated aggregates which are aligned with the close-packed $\langle 111 \rangle$ directions within the surface plane. Figure 1(b) shows the same surface area imaged at a reduced tunneling voltage of $U_t = -10$ mV and 10 MΩ tunneling resistance. Under these conditions, a wavelike surface modulation with a corrugation amplitude of ~ 0.15 Å is observed which is characterized by a periodic length of 42 Å and wave fronts aligned with the [001] direction. The wave pattern persists over the entire temperature range investigated; the only effect of temperature increase is a successive decrease in corrugation amplitude down to ~ 0.05 Å at 145 K. The overall wave pattern shows no dispersive behavior (i.e., the wavelength does not change with U_t) and appears to be largely undisturbed by steps, adsorbates, or segregated surface contaminants. Hence, it is not associated with a surface state [19] which would show the well known Friedel oscillations.

 0031-9007/00/85(16)/3500(4)$15.00

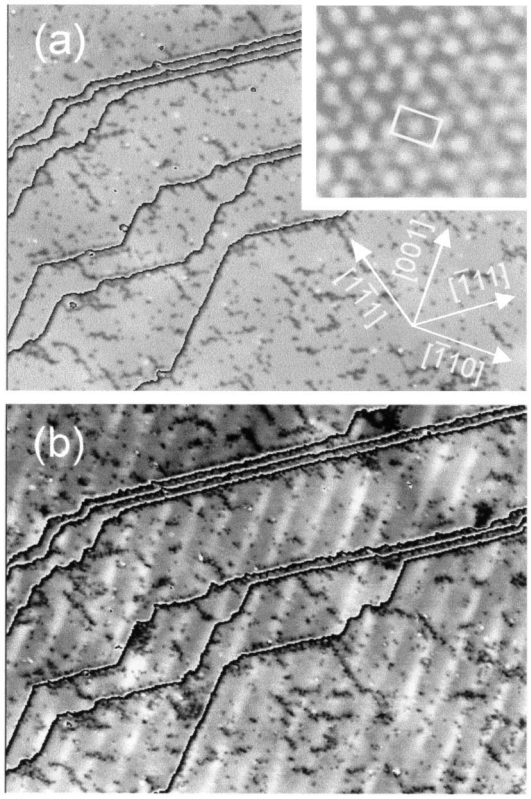

FIG. 1. (a) STM image taken at 6 K (750 Å × 560 Å, 1000 MΩ, $U_t = -1$ V) with seven Cr(110) terraces separated by monatomic steps; segregated surface contaminants are imaged as dark dots. The inset (20 Å × 18 Å, 0.1 MΩ, $U_t =$ 10 mV) demonstrates atomic resolution and shows the centered rectangular surface unit cell. (b) Same area as (a) imaged at reduced sample bias of −10 mV and 10 MΩ tunneling resistance showing a surface wave with a wavelength of 42 Å and wave fronts aligned with the [001] direction. The wave pattern is attributed to a surface charge-density modulation arising from the bulk CDW's of Cr with $\mathbf{Q} \parallel [100]$ and $\mathbf{Q} \parallel [010]$.

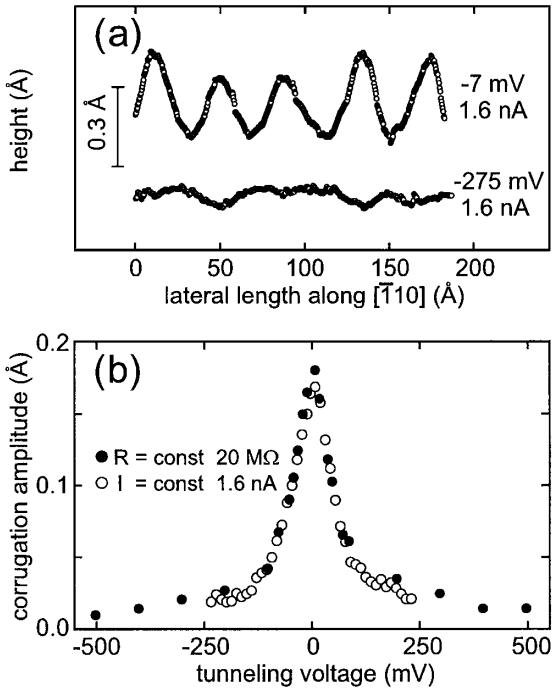

FIG. 2. Voltage-dependent magnitude of the surface wave in Fig. 1(b) at 6 K; (a) exemplary line scans 190 Å in length taken along $[\bar{1}10]$ at $U_t = -7$ mV (upper curve) and at $U_t = -275$ mV (lower curve). (b) Mean corrugation amplitude versus U_t measured at constant tunneling resistance (20 MΩ, black dots) and at constant current (1.6 nA, empty dots). The charge-density modulation is strongly enhanced for U_t below ±150 mV with respect to E_F.

By varying the sample bias we find that the wave pattern shows up for tunneling performed close to the Fermi level only; its amplitude, on the other hand, is insensitive to the tunneling resistance (i.e., the tip-sample distance) which was varied between 0.1 and 1000 MΩ. We thus conclude that the charge-density modulation observed here is not due to a topographical modulation of the surface.

The voltage-dependent magnitude of the observed wave pattern indicates that we are dealing with a surface charge-density wave coupled to the well known bulk CDW of Cr. This is apparent from Fig. 2 which illustrates the measured corrugation amplitude of the surface wave for different U_t. Figure 2(a) shows two line scans 190 Å in length taken at 6 K along the $[\bar{1}10]$ direction (i.e., perpendicular to the wave fronts). While the modulation is clearly observed at $U_t = -7$ mV with a mean amplitude of ∼0.16 Å, it is largely suppressed at $U_t = -275$ mV. We further find a continuous lateral shift of the modulation as a function of the tunneling voltage. Comparison of the line scans in Fig. 2(a) shows that the phase shift relative to the modulation measured close to E_F approaches π when the absolute value of U_t is increased. In Fig. 2(b) the mean amplitude of the surface wave is shown as a function of U_t measured at constant tunneling current ($I = 1.6$ nA, empty dots) and at a fixed tunneling resistance of 20 MΩ; see full dots (constant tunneling resistance ensures identical tip-sample distances for different U_t). In both cases the charge-density modulation is strongly enhanced for U_t below about ±150 mV and shows a pronounced maximum at E_F, demonstrating that the corrugation amplitude is solely determined by the tunneling voltage. Hence, the energetic range of electronic Cr states contributing to the observed surface wave is obviously confined to the vicinity of the Fermi energy. We interpret this characteristic feature as an unambiguous fingerprint of the CDW accompanying the SDW ground state of Cr which originates from electron and hole Fermi surface nesting [3].

Next, we verify the assignment to a surface-projected CDW on the basis of known spatial characteristics of the bulk CDW in Cr [1,2]. According to neutron and x-ray diffraction data the intrinsic bulk CDW occupies equally populated domains with the $\mathbf{Q}$ vector pointing along any of the three $\langle 100 \rangle$ lattice directions. The bulk wavelength is temperature dependent and reaches a low-temperature limit of $\lambda_{\text{bulk}} = 29.5$ Å below 20 K [5]. In contrast, the normal direction of the surface wave fronts shown in Fig. 1(b) points along the $[\bar{1}10]$ in-plane direction and the periodicity length measures 42 Å. This apparent discrepancy is

resolved by the scheme in Fig. 3 which illustrates the wave front arrangement of the three possible bulk CDW domains (labeled as **A**, **B**, and **C**) relative to the (110) surface plane. For domain **A**, planar wave fronts with $\mathbf{Q} \parallel [001]$ intersect the (110) plane at a distance identical to λ_{bulk}. On the other hand, the wave fronts connected with domains **B** and **C** ($\mathbf{Q} \parallel [010]$ and $\mathbf{Q} \parallel [100]$) produce intersection lines running along the [001] in-plane direction (see bold lines in Fig. 3) with a spacing of $\sqrt{2}\,\lambda_{\text{bulk}}$. In the temperature range from 6 to 145 K the quantity $\sqrt{2}\,\lambda_{\text{bulk}}$ amounts according to Ref. [5] to 41.7–42.9 Å, which—within the range of experimental accuracy—agrees very well with our measured value of 42 Å. The wave pattern observed here is thus identified as a surface charge-density modulation induced by the two bulk CDW domains with **Q** pointing either along the [010] or the [100] out-of-plane direction.

The major portion of our experimental data reveals surface wave patterns analogous to the exemplary case shown in Fig. 1(b). Hence, the bulk CDW with **Q** pointing along the [001] in-plane direction (cf. domain **A** in Fig. 3) appears to be largely suppressed at the Cr(110) surface. This finding is consistent with x-ray diffraction data on Cr(100) [7] and (100)-oriented Cr films [6] which show that CDW modes with **Q** oriented within the surface plane are quenched in the surface-near region. In a few cases, however, we have also detected a surface charge-density modulation connected with the remaining bulk CDW domain with **Q** parallel to the [001] in-plane direction. There is some indication that this rarely observed surface CDW is pinned by defects since it usually occurs in the vicinity of extended step bunches. Figure 4(a) shows a constant current topograph (310 Å × 190 Å, 18 MΩ, $U_t = 20$ mV, 135 K) of the related wave pattern with equidistant wave fronts running along the $[\bar{1}10]$ direction. For comparison, Fig. 4(b) reproduces the dominant surface CDW at the same scale. The crystallographic orientation of images [as indicated in Fig. 4(d)] is chosen so that wave fronts of the domain with $\mathbf{Q} \parallel [001]$ [Fig. 4(a)] are aligned vertically whereas those of the dominant domain [Fig. 4(b)] run along the horizontal direction. At the present measuring temperature, the mean corrugation of the surface CDW with $\mathbf{Q} \parallel [001]$ is about 2 times smaller compared to that found for its dominant counterpart with $\mathbf{Q} \parallel [010]$ and $\mathbf{Q} \parallel [100]$, respectively. A wave front separation of ~30 Å is deduced from Fig. 4(a) which agrees well with the expected value of λ_{bulk} for this domain labeled as **A** in Fig. 3. It is worth noting that for domain **A** no such voltage-dependent phase shift is observed as it occurs for domains **B** and **C** with $\mathbf{Q} \parallel [010]$ and $\mathbf{Q} \parallel [100]$ [cf. Fig. 2(a)]. Although we cannot yet give a definite physical explanation for the phase shift found for domains **B** and **C**, it is reasonable from the point of symmetry that no phase shift occurs for domain **A**: In this case, the planar wave fronts of the corresponding bulk CDW are oriented perpendicular to the (110) surface plane which preserves mirror symmetry with respect to the (001) plane. Figure 4(c) shows a surface area (990 Å × 810 Å, 18 MΩ, $U_t = 20$ mV, 135 K) in which the surface CDW with $\mathbf{Q} \parallel [001]$ (top right) coexists with two CDW domains with $\mathbf{Q} \parallel [010]$ or $\mathbf{Q} \parallel [100]$ (left and lower right). As a guide to the eye, respective wave front positions are depicted schematically by lines in Fig. 4(d). It is remarkable to note that the domain wall width estimated from Figs. 4(c) and 4(d) is within only a few nm. This finding corroborates previous ideas concerning domain walls in bulk Cr [20,21]: In the transversal SDW state ($\mathbf{S} \perp \mathbf{Q}$) two spin polarization domains may form for each **Q** domain. Polarization walls within single **Q** domains can be moved reversibly by external strain or magnetic fields and exhibit wall widths in the range of 100 nm [20]. Walls between SDW domains with different **Q**, on the other hand, are much harder to move and are expected to be extremely narrow (typically a few lattice constants in width [21]). Our experimental result shows that we are able to verify the latter case by direct spatial observation.

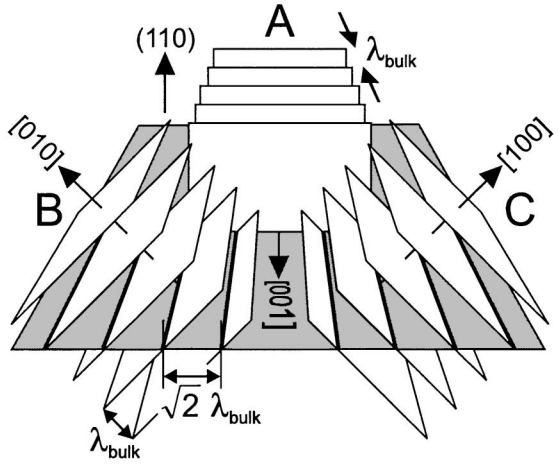

FIG. 3. Schematic wave front arrangement of the three possible bulk CDW domains of Cr (labeled as **A**, **B**, and **C**) relative to the (110) surface plane. While planar wave fronts of domain **A** ($\mathbf{Q} \parallel [001]$) intersect the (110) plane at a distance identical to the bulk wavelength λ_{bulk}, the wave fronts connected with domains **B** and **C** ($\mathbf{Q} \parallel [010]$ and $\mathbf{Q} \parallel [100]$) produce intersection lines (bold lines) running along the [001] in-plane direction with a spacing of $\sqrt{2}\,\lambda_{\text{bulk}}$.

To summarize, we have presented evidence that the bulk CDW which accompanies the SDW in Cr gives rise to significant charge-density modulations at the Cr surface. The possibility to study these modulations by LT-STM is remarkable for several reasons: First of all, the surface domain structure of Cr in its antiferromagnetic SDW ground state can be imaged and verified indirectly on the atomic scale, since the observed wave patterns are specific to the particular bulk CDW domains involved. Second, this experimental approach allows one to investigate *local* surface phenomena associated with the CDW (and thereby the

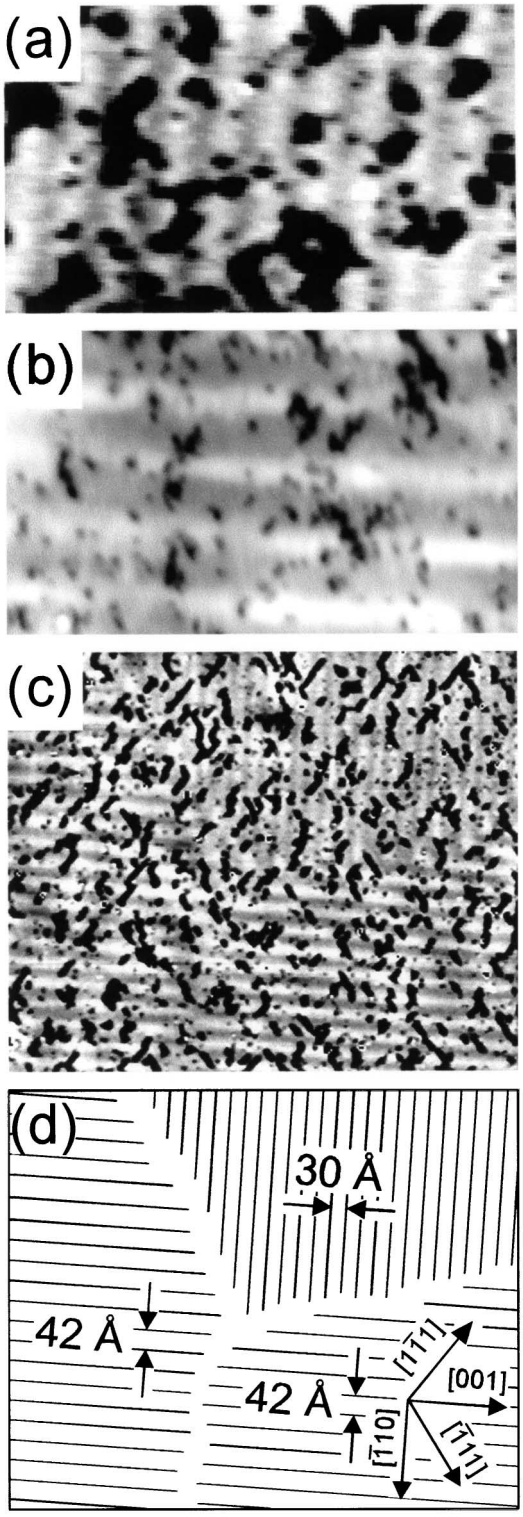

FIG. 4. (a) STM image (310 Å × 190 Å, 18MΩ, U_t = 20 mV, 135 K) showing the surface charge-density modulation arising from the bulk CDW domain with **Q** ∥ [001]; wave fronts run along the [$\bar{1}$10] direction with a spacing of ~30 Å (cf. domain **A**, Fig. 3). For direct comparison, the dominant surface CDW is reproduced in (b). (c) 990 Å × 810 Å surface area (18 MΩ, U_t = 20 mV, 135 K) in which the surface CDW with **Q** ∥ [001] (top right) coexists with two dominant CDW domains with **Q** ∥ [100] or **Q** ∥ [010], respectively (left and lower right). (d) Scheme of respective wave front positions extracted from (c). Because of enhanced contrast, surface contaminants appear more pronounced in (a) and (c) as compared to (b).

SDW) of Cr. In this context, it would be promising to probe, for example, proximity effects of ferromagnetic deposits which are expected to alter the magnetic properties of the Cr host. Furthermore, finite-size-mediated changes of the CDW in thin Cr films [6] can be studied in detail. A fascinating, however challenging, goal to achieve is the direct observation of the SDW with the help of ferromagnetic STM tips. Apart from these interesting issues, our future experiments aim at local spectroscopic measurements in order to complement the spatially averaged spectroscopic information on the SDW ground state of Cr available to date [12].

This research was supported by the Deutsche Forschungsgemeinschaft (Sfb 290, TP A5).

*Corresponding author.
Electronic address: foelsch@physik.fu-berlin.de

[1] E. Fawcett, Rev. Mod. Phys. **60**, 209 (1988), and references therein.
[2] H. Zabel, J. Phys. Condens. Matter **11**, 9303 (1999), and references therein.
[3] A. Overhauser, Phys. Rev. **128**, 1437 (1962).
[4] C. Y. Young and J. B. Sokoloff, J. Phys. F **4**, 1304 (1974).
[5] D. Gibbs, K. M. Mohanty, and J. Bohr, Phys. Rev. B **37**, 562 (1988).
[6] P. Sonntag, P. Bödeker, T. Thurston, and H. Zabel, Phys. Rev. B **52**, 7363 (1995).
[7] J. P. Hill, G. Helgesen, and D. Gibbs, Phys. Rev. B **51**, 10 336 (1995).
[8] M. N. Baibich *et al.,* Phys. Rev. Lett. **61**, 2472 (1988).
[9] P. Grünberg *et al.,* Phys. Rev. Lett. **57**, 2442 (1986).
[10] E. E. Fullerton, S. D. Bader, and J. L. Robertson, Phys. Rev. Lett. **77**, 1382 (1996); Z.-P. Shi and R. S. Fishman, Phys. Rev. Lett. **78**, 1351 (1997); A. M. N. Niklasson, B. Johansson, and L. Nordström, Phys. Rev. Lett. **82**, 4544 (1999).
[11] J. Meerschaut *et al.,* Phys. Rev. B **57**, R5575 (1998).
[12] J. Schäfer *et al.,* Phys. Rev. Lett. **83**, 2069 (1999).
[13] A. Scholl *et al.,* Science **287**, 1014 (2000).
[14] D. M. Eigler and E. K. Schweizer, Nature (London) **344**, 524 (1990).
[15] J. M. Carpinelli, H. H. Weitering, E. W. Plummer, and R. Stumpf, Nature (London) **381**, 398 (1996).
[16] H. W. Yeom *et al.,* Phys. Rev. Lett. **82**, 4898 (1999).
[17] R. V. Coleman *et al.,* Adv. Phys. **37**, 559 (1988).
[18] M. Schmid, M. Pinczolits, W. Hebenstreit, and P. Varga, Surf. Sci. **377–379**, 1023 (1997); **389**, L1140 (1997).
[19] P. E. S. Persson and L. I. Johansson, Phys. Rev. **33**, R8814 (1986).
[20] A. Hubert, *Theorie der Domänenwände in Geordneten Medien* (Springer, Berlin, 1974).
[21] E. W. Fenton, Phys. Rev. Lett. **45**, 736 (1980).